Inorganic Chemistry

ARTICLE

pubs.acs.org/IC

6-Phosphoryl Picolinic Acids as Europium and Terbium Sensitizers

Julien Andres and Anne-Sophie Chauvin*

École Polytechnique Fédérale de Lausanne, ISIC, BCH 1405, CH-1015 Lausanne, Switzerland

Supporting Information

ABSTRACT: Three 6-phosphoryl picolinic acid (6PPA) derivatives were synthesized and used as europium and terbium sensitizers. Two of the three ligands (6-diethoxyphosphoryl picolinic acid (Hdeppa) and 6-monoethoxyphosphoryl picolinic acid (H_2meppa)) are water-soluble, once complexed to lanthanide ions, while the third (6-dihydroxyphosphoryl picolinic acid (H_3dhppa)) forms a precipitate. The stability constants of the phosphoryl-based complexes were found to be higher than the carboxylate analogue (dipicolinic acid, H_2dpa). The main species are the $[LnL_3]$ complexes under strict stoichiometric conditions, confirmed by ^{31}P NMR spectroscopy, mass spectrometry and lifetime analyses. The photophysical measurements reveal that the emission intensity of $[Eu(deppa)_3]$ is maximal at pH 4.8, whereas for $[Eu(meppa)_3]^{3-}$, the optimum pH is observed at 9.0. The lifetimes are all in the millisecond range and have confirmed the absence of water molecules in the first coordination sphere. The emissions of the terbium are always brighter than the corresponding europium within this phosphoryl series. The quantum yields of the phosphoryl containing complexes are lower than the carboxylate analogue ($[Ln(dpa)_3]^{3-}$), except for $[Tb(deppa)_3]$, which exhibits an interesting quantum yield of 40% in aqueous solution.

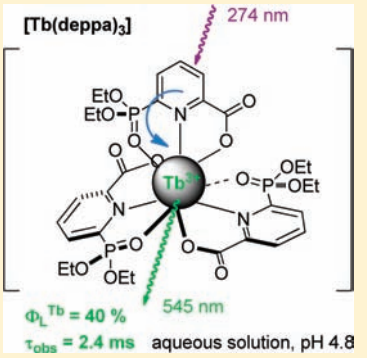

INTRODUCTION

The use of lanthanides complexes has extensively grown during the past decade, especially because of their luminescence properties (i.e., narrow bands, long lifetimes, no photobleaching).[1−3] Coordinating ligands with various shapes and structures are used both to sensitize the luminescent cations and prevent the non-radiative deactivations.[4] Among these ligands, a framework based on dipicolinic acid has come out as a very versatile and efficient coordinating and sensitizing moiety. Its derivatization has been extensively investigated and is observed to be often detrimental to the luminescence properties.[5−7] Nevertheless, most of these derivatizations focus on extending the absorption range by coupling with additional chromophores. A recent evolution in this field was undertaken with a spatial decoupling of the chromophoric unit and the coordinating moiety, thus allowing changing the nature of the chromophoric unit with no impact on the coordination moiety.[8]

The strong importance of the dipicolinic framework can not only be explained by its very good photophysical properties for luminescent lanthanide sensitization, but also is attributable to the quick complexation with lanthanide cations and high stability of the tris complex. Therefore, a dipicolinic moiety is also a good coordinating group when it comes to ligand design, especially for obtaining tris complexes.

Although most of the ligands designed for lanthanide ions are coordinating to the metal with a carboxylate moiety (e.g., polyaminocarboxylates) or at least a carbonyl (e.g., β-diketonates), some other functional groups have also gained some interest.[9] Among them, phosphoryl groups such as phosphonate or phosphoesters have been shown to usually enhance the stability with a similar complexation mode, compared to a carboxylate analogue (for instance, when comparing 1,4,7,10-tetraazacyclododecane-1,4,7-triacetic acid (H_3do3a), 1,4,7,10-tetraazacyclododecane-1,4,7,10-tetraacetic acid (H_4dota), and H_4dota-like ligands).[10,11] Furthermore, phosphonates have shown a few interests for applications in magnetic resonance imaging (MRI) with Gd^{3+} complexes, but also as an anchoring group for targeting bones or TiO_2 nanoparticles.[12,13]

We propose to investigate the influence of the coordinating groups on the dipicolinic framework by replacing one of the carboxylic acid of dipicolinic acid by a phosphoryl derivative (diethoxy, monoethoxy, or dihydroxy phosphoryl). The choice of phosphoryl coordinating units is justified by their known cationic affinity and by the little documentation about their effect on the luminescence properties of trivalent lanthanide cations.[14−17] Here, we report the synthesis of three 6-phosphoryl picolinic acids as ligands for lanthanide complexes. We study their stabilities and photophysical properties, and we compare them to those of europium and terbium trisdipicoliniate complexes. Interestingly, the entire series of ligands (i.e., 6-phosphoryl picolinic acids and dipicolinic acid) is water-soluble, thus allowing a direct comparison of the complex properties in the same conditions. Figure 1 shows the general structure of dipicolinic acid (H_2dpa), diethoxyphosphoryl picolinic acid (Hdeppa), monoethoxyphosphoryl picolinic acid (H_2meppa), and dihydroxyphosphoryl picolinic acid (H_3dhppa).

Received: May 10, 2011
Published: September 22, 2011

dx.doi.org/10.1021/ic200983y | Inorg. Chem. 2011, 50, 10082–10090

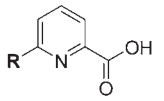

R = COOH H_2dpa
R = $PO(OEt)_2$ Hdeppa
R = PO(OEt)OH H_2meppa
R = $PO(OH)_2$ H_3dhppa

Figure 1. Structure of the ligands: dipicolinic acid (H_2dpa), diethoxyphosphoryl picolinic acid (Hdeppa), monoethoxyphosphoryl picolinic acid (H_2meppa), and dihydroxyphosphoryl picolinic acid (H_3dhppa).

EXPERIMENTAL SECTION

General Procedures. The solvents were purified by a nonhazardous procedure by passing them through activated alumina columns (Innovative Technology, Inc.).[18] The chemicals were ordered from Fluka and Aldrich and used without further purification. The electrospray ionization mass spectrometry (ESI-MS) spectra were obtained on a Finningan Model SSQ 710C spectrometer, using 10^{-5}−10^{-4} M solutions in acetonitrile/H_2O/acetic acid (50/50/1) or MeOH, a capillary temperature of 200 °C and an acceleration potential equal to 4.5 keV. The instrument was calibrated using a horse myoglobin standard, and the analyses were conducted in positive mode with a 4.6 keV ion spray voltage. The elemental analyses were performed by Dr. E. Solari at the École Polytechnique Fédérale de Lausanne. Nuclear magnetic resonance (^{1}H and ^{31}P NMR) spectroscopy were performed on a Bruker Model Avance DRX 400 spectrometer, and ^{13}C NMR spectroscopy was performed on a Bruker Model AV 600 MHz at 25 °C, using deuterated solvents as internal standards. The chemical shifts are given in parts per million (ppm), relative to tetramethylsilane ($SiMe_4$). High-performance liquid chromatography (HPLC) was performed on a Waters Model 600 apparatus (pump and controller) with a Waters Model 2487 dual λ absorbance detector using a reverse-phase column (Model Symmetry C_{18}, 3.5 μm, 4.6 mm × 75 mm) with an acetonitrile/water eluent starting from 0% acetonitrile and increasing by 1% per minute at a flow rate of 1 mL min^{-1}.

Synthesis of the Ligands. *6-Diethoxyphosphoryl Picolinic Acid (Hdeppa).* Hdeppa was synthesized according to a known procedure,[14] starting from ethylpicolinate. The pure pale solid was obtained in 34% yield from the starting material. HPLC analysis showed the presence of one compound, with a retention time of 21.6 min. ^{1}H NMR (400 MHz, D_2O) δ, ppm: 8.17 (d, J = 7.4 Hz, 1 H), 8.07 (m, 2 H), 4.15 (m, 4 H), 1.24 (t, J = 7.1 Hz, 6 H). ^{13}C NMR (126 MHz, D_2O) δ, ppm: 167.7 (s, $\underline{C}$OOH), 150.0 (d, J = 151.9 Hz, $\underline{C}_{pyr6}$−P), 149.0 (d, J = 53.4 Hz, $\underline{C}_{pyr2}$−C), 139.7 (d, J = 11.8 Hz, $\underline{C}H_{pyr4}$), 132.1 (d, J = 24.8 Hz, $\underline{C}H_{pyr5}$), 128.8 (d, J = 3.6 Hz, $\underline{C}H_{pyr3}$), 65.8 (d, J = 5.6 Hz, O-$\underline{C}H_2$−C), 16.9 (d, J = 5.7 Hz, C−$\underline{C}H_3$). ^{31}P NMR (162 MHz, D_2O) δ, ppm: 12.5 (s). Anal. Calcd for $C_{10}H_{14}NO_5P$: 46.34% C, 5.44% H, 5.40% N; Found: 46.62% C, 5.47% H, 5.35% N.

6-Monoethoxyphosphoryl Picolinic Acid (H_2meppa). 0.1 M Sodium hydroxide (1.3 mmol, 13 mL), was added to a solution of 6-diethoxyphosphoryl picolinic acid (1.3 mmol, 337 mg) in water (32.5 mL) at room temperature. After stirring for 1 h, another equivalent of 0.1 M sodium hydroxide (1.3 mmol, 13 mL) was added. The reaction was completed after 1.5 h, as shown by ^{31}P NMR spectroscopy. The aqueous phase was washed three times with CH_2Cl_2 (3 × 60 mL) and acidified by 0.1 M HCl down to pH 1.5. No precipitation was observed. After evaporation of the solvent under reduced pressure, the precipitation of salts was performed by addition of MeOH (2 mL). Evaporation of the filtrate under reduced pressure and further precipitation of salts were repeated three times to obtain H_2meppa in the form of a brownish transparent oil (233 mg, 78%). HPLC analysis showed the presence of one compound with a retention time of 8.0 min. ^{1}H NMR (400 MHz, D_2O) δ, ppm: 8.44 (m, 1 H), 8.32 (d, J = 8.0 Hz, 1 H), 8.17 (t, J = 7.3 Hz, 1 H), 3.89 (m, 2 H), 1.14 (t, J = 7.1 Hz, 3 H). ^{13}C NMR (126 MHz, D_2O) δ, ppm: 163.9 (s, $\underline{C}$OOH), 152.9 (d, J = 178.7 Hz, $\underline{C}_{pyr6}$−P), 146.6 (d, J = 8.0 Hz, $\underline{C}_{pyr2}$−C), 143.1 (d, J = 9.2 Hz, $\underline{C}H_{pyr4}$), 131.3 (d, J = 13.0 Hz, $\underline{C}H_{pyr5}$), 127.8 (s, $\underline{C}H_{pyr3}$), 65.1 (O−$\underline{C}H_2$−C), 14.7 (s, C−$\underline{C}H_3$). ^{31}P NMR (162 MHz, D_2O) δ, ppm: 9.20 (s). Anal. Calcd for $C_8H_{10}NO_5P \cdot 2HCl$: 31.60% C, 3.98% H, 4.61% N; Found: 31.52% C, 3.56% H, 4.26% N.

6-Dihydroxyphosphoryl Picolinic Acid (H_3dhppa). 6-Monoethoxyphosphoryl picolinic acid (0.65 mmol, 150 mg) was dissolved in water (5 mL), and 5 M sodium hydroxide (10 mmol, 2 mL) was added. The solution was refluxed for 6 h. The solvent was then progressively evaporated to push the equilibrium toward the formation of the desired product. The procedure was repeated once more until completion of the reaction as shown by ^{31}P NMR spectroscopy. The crude product was dissolved in water (25 mL), and the aqueous phase was washed three times with CH_2Cl_2 (3 × 25 mL). The aqueous phase was then acidified with 0.1 M HCl down to pH 1.5 without any precipitation of the product. After evaporation of the solvent under reduced pressure, the precipitation of salts was performed in MeOH similarly to H_2meppa and gave H_3dhppa as a pale brownish hygroscopic powder (86 mg, 63%). The HPLC analysis showed the presence of one compound with a retention time of 1.1 min. ^{1}H NMR (400 MHz, D_2O) δ, ppm: 7.80−7.72 (m). ^{13}C NMR (126 MHz, D_2O) δ, ppm: 163.7 (s, $\underline{C}$OOH), 152.9 (d, J=178.6 Hz, $\underline{C}_{pyr6}$−P), 146.6 (d, J = 8.9 Hz, $\underline{C}_{pyr2}$−C), 145.3 (d, J = 9.6 Hz, $\underline{C}H_{pyr4}$), 131.5 (d, J = 13.2 Hz, $\underline{C}H_{pyr5}$), 128.0 (s, $\underline{C}H_{pyr3}$). ^{31}P NMR (162 MHz, D_2O) δ, ppm: 6.90 (s). Anal. Calcd for $C_6H_6NO_5P \cdot 0.25NaCl \cdot 1.1$ MeOH: 31.02% C, 3.45% H, 5.10% N; Found: 31.09% C, 3.34% H, 5.17% N.

Physicochemical Measurements. *Spectrophotometric Measurements.* The analytical-grade solvents and chemicals were used without further purification. The aqueous solutions were prepared from doubly distilled water. The lanthanide solutions were prepared from the corresponding perchlorate salt and were titrated by complexometry, using a standardized Na_2H_2EDTA solution in urotropine-buffered medium and with Xylenol Orange as an indicator.[19]

The ultraviolet−visible light (UV−vis) absorption spectra were measured on a Perkin−Elmer Model Lambda 900 spectrophotometer using 1-cm-path-length quartz cells. The spectrophotometric titrations were performed with a J&M diode array spectrometer (Tidas series) connected to an external computer. All titrations were performed in a thermostatted (25.0 °C) glass-jacketed vessel and in a 0.1 M solution in KCl. In a typical ligand titration experiment, as a function of pH, 25 mL of a 3 × 10^{-5} M ligand solution was titrated with a standardized 0.1 M NaOH solution. The pH of the solution was continually measured with a freshly calibrated 3.0 M KCl electrode to ensure the pH value after base addition was stable. A UV−vis spectrum using a Hellma optrode (optical path length of 1 cm) connected to the Tidas spectrometer and immersed in the thermostatted vessel was then recorded once the pH value was stable. The procedure was repeated to measure the absorption each 0.2−0.4 pH unit. Since the titrations were performed with a base addition, the solutions were previously acidified with HCl until the absorption spectra do not change anymore (pH 1−2).

The factor analysis and mathematical treatment of the spectrophotometric data were performed with the SPECFIT program.[20]

NMR Measurements. The titrations of the ligands with Lu^{3+} were performed via the addition of 2 μL of a 0.0825 M $Lu(ClO_4)_3$ solution in D_2O to 0.5 mL of a 3 × 10^{-3} M solution of the ligand in D_2O (0.11 equiv of Lu^{3+} per addition). The ^{1}H and ^{31}P NMR spectra were recorded on a Bruker Model Avance DRX 400 spectrometer.

Luminescence Measurements. The luminescence measurements were recorded on a Fluorolog 3-22 spectrofluorimeter from Jobin−Yvon. The emission and excitation spectra were measured in 1-cm-path-length quartz cells at room temperature and in quartz Suprasil capillaries at 77 K with 10% glycerol added to the solutions. All emission spectra were

measured in photon counts and corrected for the instrumental function. The luminescence evolution of the europium complexes was performed by variation of the pH (similar to the titration of the ligands, but in a 1:3 europium/ligand solution).

The quantum yields were measured comparatively to europium or terbium trisdipicolinate aqueous solutions in Tris-HCl 0.1 M at pH 7.4, which exhibit a quantum yield of 24% or 22%, respectively.[21] All concentrations were set at 1×10^{-4} M, including the concentration of the reference trisdipicolinate complexes. The excitation wavelength was chosen where the absorption spectra of the reference and of the sample cross to ensure an identical amount of absorbed quanta.

Equation 1 describes the quantum yield calculation in nondiffusing solutions:

$$\Phi_{em} = \frac{\int_{\lambda_{em}} I_{em}^{sample}(\lambda)\,d\lambda}{\int_{\lambda_{abs}} I^0(\lambda)(1 - T^{sample}(\lambda))\,d\lambda} \frac{\int_{\lambda_{abs}} I^0(\lambda)(1 - T^{ref}(\lambda))\,d\lambda}{\int_{\lambda_{em}} I_{em}^{ref}(\lambda)\,d\lambda} \Phi_{em}^{ref}$$

$$= \frac{\int_{\lambda_{em}} I_{em}^{sample}(\lambda)\,d\lambda}{\int_{\lambda_{em}} I_{em}^{ref}(\lambda)\,d\lambda} \Phi_{em}^{ref}$$

$$\Leftrightarrow \int_{\lambda_{abs}} I^0(\lambda)(1 - T^{sample}(\lambda))\,d\lambda = \int_{\lambda_{abs}} I^0(\lambda)(1 - T^{ref}(\lambda))\,d\lambda \quad (1)$$

where $I_{em}(\lambda)$ is the emission spectrum of the sample or reference, $I^0(\lambda)$ the incoming excitation light spectrum, and $T(\lambda)$ the transmittance of the sample or reference.

The radiative lifetimes (τ_r), intrinsic quantum yields (Φ_{Ln}^{Ln}), and sensitization efficiency (η_{sens}) were calculated according to the expressions given in eqs 2a−c:[22]

$$\frac{1}{\tau_r} = k_r = A_{MD,0}\, n^3 \left(\frac{I_{tot}}{I_{MD}}\right) \quad (2a)$$

$$\Phi_{Ln}^{Ln} = \frac{\tau_{obs}}{\tau_r} \quad (2b)$$

$$\Phi_{em} = \Phi_L^{Ln} = \eta_{sens} \Phi_{Ln}^{Ln} \quad (2c)$$

Here, k_r is the radiative de-excitation rate, τ_{obs} is the observed lifetime upon radiative and nonradiative deactivation, and $A_{MD,0}$ is the spontaneous emission probability for the purely magnetic dipole (MD) transition, whose intensity is practically not influenced by the chemical environment of the lanthanide ion ($^5D_0 \rightarrow {}^7F_1$ in Eu^{3+}; $A_{MD,0} = 14.65\ s^{-1}$). In addition, n is the refractive index of the solvent and I_{tot}/I_{MD} is the ratio of total emission intensity over emission intensity of the MD transition.

Water molecules in the first coordination sphere have been estimated by the Supkowski and Horrock formula, given by eq 3a and 3b:[23]

$$q = A\left[\tau_{obs}{}^{-1}(H_2O) - \tau_{obs}{}^{-1}(D_2O) - k_{XH}\right] \quad (3a)$$

$$k_{XH} = \alpha + \beta\, n_{OH} + \gamma\, n_{NH} + \delta\, n_{O=CNH} \quad (3b)$$

where $\tau_{obs}(H_2O)$ is the lifetime in water, $\tau_{obs}(D_2O)$ the lifetime in deuterated water, n_{XH} the number of XH oscillators in the first coordination sphere, α the contribution of the water molecules in the outer coordination sphere, β the contribution of an OH oscillator in the first coordination sphere, γ the contribution of a NH oscillator in the first coordination sphere, and δ the contribution of a O=CNH oscillator in the first coordination sphere.

The high-resolution excitation spectrum of the $^5D_0 \leftarrow {}^7F_0$ transition was measured by exciting the sample from 579.39 nm to 581.38 nm with a tunable rhodamine 6G dye laser (Coherent CR-599 dye laser, band pass = 0.03 nm, 50−300 mW) pumped with an argon CW laser at 514 nm (Coherent Innova-90 argon laser, 8 W). The sample was frozen at 12 K in a CTI-Cryogenics Cryodyne M-22 closed-cycle refrigerator controlled by a Lakeshore 321 temperature controller. Ten percent (10%) glycerol was previously added to the aqueous solution, to prevent an excessive dilatation once frozen. The excitation wavelength was calibrated with a Spex 1404 double monochromator with holographic gratings (band pass = 0.01−0.02 nm) and the emission intensity of the $^5D_0 \rightarrow {}^7F_2$ transition at 615 nm was monitored at 90° with a Hamamatsu Model R943-02 photomultiplier with a cooled S-20 photocatode (−20 °C) coupled to a Model DC-440 MHz wideband homemade amplifier (25× amplifier) and a Stanford Research Model SR-400 double-photon counter.

Table 1. Acid Dissociation Constants of the 6PPA Ligands[a]

	H_2dpa[b]	Hdeppa	H_2meppa	H_3dhppa
pK_{a1}	0.5(2)	3.07(4)	3.41(9)	2.2(3)
pK_{a2}	2.03(1)	7.0(1)	4.4(2)	3.06(9)
pK_{a3}	4.49(1)		6.4(2)	7.07(8)
pK_{a4}				7.53(9)

[a] In 0.1 M KCl aqueous solution at 25 °C. [b] Data obtained from ref 24.

RESULTS AND DISCUSSION

Acido-Basic Properties of the Ligands. The number of protonation sites among the phosphoryl ligands is not constant. The difference is dictated by the phosphoryl moiety. The dihydroxyphosphoryl (i.e., phosphonic acid) group has two protonation sites and the monoethoxyphosphoryl has only one protonation site, whereas the diethoxyphosphoryl does not possess any protonation site. The rest of the molecule is identical, with two additional protonation sites: either a pyridine that can be protonated to give a pyridinium or a carboxylate that can be protonated to give a carboxylic acid. Hence, the influence of the phosphoryl substituents on the rest of the molecule may give useful pieces of information to help better understand the physicochemical properties of the ligands and their complexes. Equation 4 shows the equilibria involved in protonation in water:

$$H_2deppa^+ + H_2O \overset{K_{a1}}{\rightleftharpoons} Hdeppa + H_3O^+$$
$$Hdeppa + H_2O \overset{K_{a2}}{\rightleftharpoons} deppa^- + H_3O^+$$
$$H_3meppa^+ + H_2O \overset{K_{a1}}{\rightleftharpoons} H_2meppa + H_3O^+$$
$$H_2meppa + H_2O \overset{K_{a2}}{\rightleftharpoons} Hmeppa^- + H_3O^+$$
$$Hmeppa^- + H_2O \overset{K_{a3}}{\rightleftharpoons} meppa^{2-} + H_3O^+$$

$$H_4dhppa^+ + H_2O \overset{K_{a1}}{\rightleftharpoons} H_3dhppa + H_3O^+$$
$$H_3dhppa + H_2O \overset{K_{a2}}{\rightleftharpoons} H_2dhppa^- + H_3O^+$$
$$H_2dhppa^- + H_2O \overset{K_{a3}}{\rightleftharpoons} Hdhppa^{2-} + H_3O^+$$
$$Hdhppa^{2-} + H_2O \overset{K_{a4}}{\rightleftharpoons} dhppa^{3-} + H_3O^+ \quad (4)$$

The absorption spectra of Hdeppa, H_2meppa, and H_3dhppa were collected at different pH values, and these data were used to fit the pK_a values (see Table 1), using SPECFIT (see Figures S1−S3 in the Supporting Information). Protonation models with two, three and four pK_a values were used. The reconstructed distribution diagrams are shown in Figures S4−S6 in the Supporting Information.

The pK_a values, obtained from the UV−vis absorption spectra, correlates with the values obtained for other phosphonic acids, based on related structures.[14,15] According to the acidic nature of the carboxylic acid and basic behavior of the pyridine, the two pK_a values found for Hdeppa are attributed to the deprotonation of the carboxylic acid concerning the pK_{a1} = 3.07

dx.doi.org/10.1021/ic200983y |Inorg. Chem. 2011, 50, 10082–10090

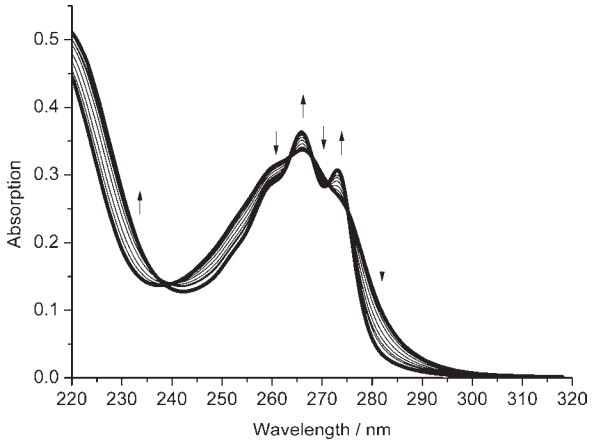

Figure 2. UV−vis spectrophotometric titration of a 9.0×10^{-5} M aqueous solution of Hdeppa in KCl 0.1 M with Eu^{3+}, pH 4.8, 298 K. Arrows indicates the evolution upon the addition of Eu^{3+}.

($H_2deppa^+ \leftrightarrows$ Hdeppa) and to the deprotonation of the pyridinium nitrogen to form the pyridine for the $pK_{a2} = 7.0$ (Hdeppa $\leftrightarrows$ $deppa^-$). Similarly, the pK_{a1} value of H_2meppa (3.41), was attributed to the carboxylic acid ($H_3meppa^+ \leftrightarrows H_2meppa$), and the pK_{a2} value was attributed to the monoethyl ether phosphonic acid (4.4) ($H_2meppa \leftrightarrows Hmeppa^-$); the pK_{a3} value was attributed to the pyridine nitrogen (6.4) ($Hmeppa^- \leftrightarrows meppa^{2-}$). Concerning the four protonation sites of H_3dhppa, the attribution of the acidic pK_a values is intricate. Usually, phosphonic acids are more acidic than their carboxylic analogues[25] Nevertheless, the ^{31}P NMR chemical shifts of the ligand in 0.1 M D_2SO_4, D_2O, or 0.1 M NaOD (see Table S1 in the Supporting Information) show that the peak of the phosphorus nucleus is more shifted by the removal of a proton from H_3dhppa than by the removal of a proton from H_4dhppa^+. Such higher shifts of the ^{31}P NMR chemical shift may be expected for the removal of phosphonic protons separated by only two chemical bonds from the phosphorus, whereas the removal of the far carboxylic proton should affect the chemical environment should affect to a lesser extent the chemical environment of the phosphorus. For example, the ^{31}P NMR chemical shift of Hdeppa is only shifted from 12.5 ppm to ±0.7 ppm by the addition of the carboxylic proton or the removal of the pyridinium proton. On the other hand, the increased capability of H_2dhppa to form hydrogen bonds may also have a significant influence on the chemical shifts. Therefore, only the pK_{a3} value of 7.07 can be easily assigned to the pyridine core ($H_2dhppa^- \leftrightarrows Hdhppa^{2-}$) and the pK_{a4} value of 7.53 to the second deprotonation of the phosphonic acid ($Hdhppa^{2-} \leftrightarrows dhppa^{3-}$). The pK_{a1} and pK_{a2} values are tentatively assigned to the carboxylic acid and the phosphonic acid, respectively.

As a result, the main influence of a phosphoryl coordinating moiety (diethoxy, monoethoxy, or diethoxyphosphoryl) on the acido-basic properties of such ligands is a much more basic pyridine in all the phosphoryl ligands, compared to dipicolinic acid. A difference of at least 2 pK_a units is observed. This has a dramatic effect on the distribution diagrams of the phosphoryl ligands (see Figures S4−S6 in the Supporting Information). Because the full deprotonation of dipicolinic acid requires a pH higher than 7.0, the deprotonation of the pyridinium in all phosphoryl ligands needs a pH higher than 9.0.

Stoichiometry and Stability of the Ln Complexes. UV−vis spectrophotometric titrations were performed to observe the formation of the europium complexes. To a 9.0×10^{-5} M aqueous solution of ligand in 0.1 M KCl, increasing amounts of europium perchlorate were added, up to more than 1 equiv of Eu^{3+} ions. The pH of the solution was kept at 4.8 for Hdeppa and 9.0 for $meppa^{2-}$ via the addition of HCl and NaOH solutions. These pH values will be shown to be optimal for luminescence. Concerning H_3dhppa, the formation of a precipitate was observed upon the addition of lanthanide salts. The stability constants are then undetermined for this ligand. Interestingly, all the ligands are water-soluble, but only $deppa^-$ and $meppa^{2-}$ form water-soluble complexes. Here, a highly charged ligand such as $dhppa^{3-}$ is disadvantageous, since precipitation occurs in the presence of lanthanide ions, whereas the uncharged $[Ln(deppa)_3]$ complex is very soluble in water.

A better definition of the absorption bands is observed for the two titrated ligands upon the addition of Eu^{3+} ions, as seen in Figure 2 and Figure S7 in the Supporting Information. This behavior might come from the restricted vibrational modes of the ligand when it is coordinated to the lanthanide ion.

The titration of Hdeppa shows a neat growth of its two absorption peaks at 273 and 266 nm, whereas the remaining shoulder at 260 nm decreases when the concentration of europium increases. Five isosbestic points have emerged at 275, 271, 268, 264, and 239 nm.

Concerning H_2meppa, the evolution of the absorption spectrum upon addition of the europium salt is more intricate (see Figure S7 in the Supporting Information). Although a similar evolution as Hdeppa is observed up to 0.33 equiv with a slight bathochromic shift of 1 nm upon europium addition (see Figure 2), an increase of absorption at the local minimum between 240 and 250 nm, at the maxima at 275 and 268, as well as at the shoulder at 262 nm is observed up to 0.5 equiv. The minimum then keeps growing, whereas the maxima decrease even below the absorption at 0.33 equivalent. One isosbestic point is defined at 280 nm, the other crossings being either poorly defined or only valid for part of the spectra.

Equation 5 gives the equilibria for the complex formation (charge omitted):

$$\begin{aligned} Ln + L &\xrightleftharpoons{\beta_{[LnL]}} [LnL] \\ Ln + 2L &\xrightleftharpoons{\beta_{[LnL_2]}} [LnL_2] \\ Ln + 3L &\xrightleftharpoons{\beta_{[LnL_3]}} [LnL_3] \end{aligned} \qquad (5)$$

The fitting with SPECFIT of the absorption spectra of both ligands gives the $\log \beta$ values shown in Table 2. The distribution diagram of the species formed during the titration of Hdeppa by Eu^{3+} is shown in Figure 3. The fitting of the absoption spectra of the $[Eu(deppa)_n]^{3-n}$ species needed a fixed $\log \beta_{[LnL]}$ value to converge toward reasonable reconstructed absorptivities. A value of 8.0 was found to give satisfactory results and seems rational, by comparison with the stability constants of $[Eu(dpa)_n]^{3-2n}$ measured under comparable conditions with the same technique.[21] The fitting of the absoption spectra of the $[Eu(meppa)_n]^{3-2n}$ species was not as good as the fitting for the $[Eu(deppa)_n]^{3-n}$ species. Although the values presented in Table 2 yielded realistic reconstructed absorptivities for every species, the $\log \beta$ values are to be taken cautiously.

Despite the limits of the fitting procedure, the similar stability constants (within experimental error) for all $[Eu(deppa)_n]^{3-n}$ and the $[Eu(meppa)_n]^{3-2n}$ ($n \in [1,3]$) stoichiometries suggest

Table 2. Stability Constants of the Complexes (in KCl 0.1 M, 298 K)

	H_2dpa,[a] pH 7.4	Hdeppa, pH 4.8	H_2meppa, pH 9.0
log $\beta_{[EuL]}$	8.7(3)	8.0 (fixed)	8.2(4)
log $\beta_{[EuL2]}$	16.8(3)	16.2(2)	16.0(5)
log $\beta_{[EuL3]}$	22.4(3)	23.8(2)	24.3(4)

[a] Data taken from ref 21.

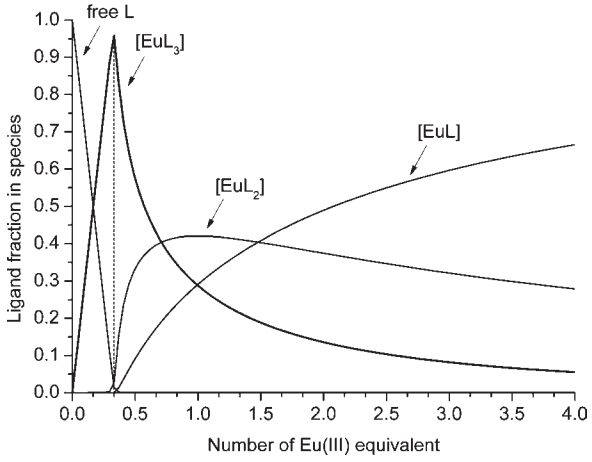

Figure 3. Distribution diagram of the species formed during the titration of Hdeppa by Eu^{3+} in KCl 0.1 M, pH 4.8, 298 K. Dashed line indicates the maximum of the 1:3 species at 0.33 equiv.

that the phosphoryl substituents (i.e., a $PO(OEt)_2$ versus a PO(OEt)OH) have no strong effect on the coordination strength or coordination mode. However, relative to the $[Eu(dpa)_n]^{3-2n}$ complexes, the 1:3 species of the phosphoryl analogues seem more stable than the parent carboxylate, similar to that which what have already been observed with other phosphoryl-based ligands.[15] The increased stability, compared to $[Ln(dpa)_n]^{3-2n}$ complexes can be rationalized by the increased basicity of all the coordinating groups in the 6-phosphoryl picolinate series. A strong base is usually a good coordinating group, because of its better electron-donating ability (by definition, a base is an electron donor, according to Lewis's definition of acids and bases).

The stability of such complexes is dependent on the pH. We chose to set a different pH for each complex, because these values are demonstrated to be optimal for luminescence in the next section.

To further check the presence of a 1:3 complex being the main species in solution, NMR experiments were conducted. The ligands were dissolved in D_2O and titrated by Lu^{3+}. ^{31}P NMR spectroscopy was found to be really useful, exhibiting different signals for each species (both proton speciation of the ligands and complex species).

This is particularly true for the Hdeppa ligand that shows a defined peak at 0.33 equiv of Lu^{3+} (Figure 4). During the titration of Hdeppa by Lu^{3+}, an evolution of the ligand single peak at 12.5 ppm is observed upon addition of the lanthanide salt. The ligand peak decreases in intensity as soon as lutetium is added. A new peak consistent with the appearance of $[Lu(deppa)_3]$ forms at ~20 ppm and remains for lutetium amounts from 0.33 equiv to 0.44 equiv. It then begins to decrease in agreement with the decrease of the 1:3 species concentration. A new broad peak appears then between 20 and 21 ppm before a defined peak

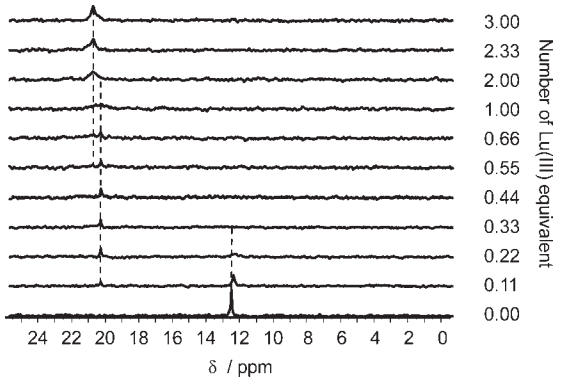

Figure 4. ^{31}P NMR spectrum of 3×10^{-3} M Hdeppa in D_2O, titrated by Lu^{3+}, pD ~5.4.

Table 3. Main Peaks of the ElectroSpray Ionization Time-of-Flight Mass Spectrometry (ESI-TOF-MS) Analysis of the $[Eu(deppa)_3]$ Complex in Water

species	m/z (obs)	m/z (calcd)
$[Eu(deppa)_3 + 2H^+]$	464.71	464.55
$[Eu(deppa)_3 + 1H^+]$	928.39	928.09
$[Eu(deppa)_2]^+$	669.23	669.02

emerges from the broad one and keeps growing as the concentration of the $[Ln(deppa)]^{2+}$ species increases.

The H_2meppa spectrum, on the other hand, is poorly defined at 0.33 equiv of lutenium (see Figure S9 in the Supporting Information). A peak at 15 ppm is observed at metal concentrations higher than 0.33 equiv of lutetium, and a progressive decrease of the free ligand peaks at 3 ppm and 7.9 ppm (two protonated species are present at this pD value) is encountered up to 0.33 equiv of lutetium. This experiment did not directly enable visualizing the formation of a major $[Lu(meppa)_3]^{3-}$ species, but the evolution of the other species associated with the observed ^{31}P NMR peaks suggests that a 1:3 complex form at 0.33 equiv of lutetium, similar to that observed for $[Lu(deppa)_3]$. The 1:3 stoichiometry was further tested by mass spectrometry. Some europium perchlorate and the appropriate amount of ligand were dissolved in distilled water, keeping a strict 1:3 concentration ratio, and the resulting solution was injected in an electrospray mass spectrometer within a micromolar concentration range.

The $[Eu(deppa)_3]$ complex was detected as monoprotonated and biprotonated tris species (see Table 3 and Figure S10 in the Supporting Information). The isotopic distributions of the measured species are in agreement with the calculated distributions expected for these complexes.

Peaks corresponding to $[Eu(meppa)_2]^-$ have been measured, but no tris species was observed with this method. It may be due to the conditions required for mass spectrometry (i.e., the detection of complexes in negative mode being somewhat more difficult than detection in positive mode). However, because luminescence-based methods, presented in the photophysical properties section, have proved the formation of a nonhydrated coordination sphere in $meppa^{2-}$ complexes at pH 9.0 upon a metal:ligand ratio of 1:3, the ligand-filled coordination sphere that corresponds to the 1:3 species should be the major species.

Luminescence as a Function of pH. The emission spectra of $[Eu(deppa)_3]$ and $[Eu(meppa)_3]^{3-}$ were measured as a function

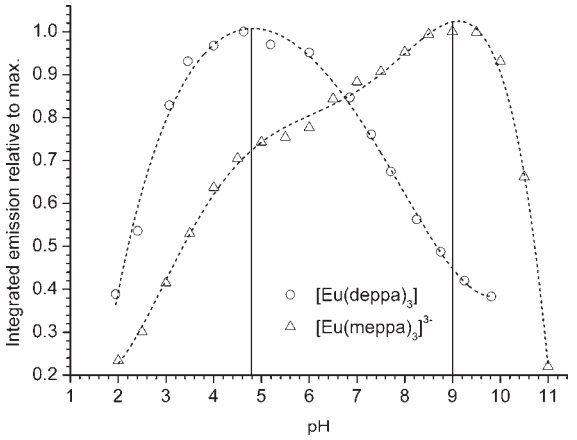

Figure 5. Normalized integrated emission intensity of (○) $[Eu(deppa)_3]$ and (△) $[Eu(meppa)_3]^{3-}$, as a function of pH. Concentration of the complex (either $[Eu(deppa)_3]$ or $[Eu(meppa)_3]^{3-}$): 1×10^{-4} M in KCl 0.1 M aqueous solution, 298 K. Solid lines are drawn to indicate the chosen pH values resulting in a maximal emission of the considered complex.

of pH. The integration of the emission and the normalization, relative to the maximal integrated intensity, results in Figure 5. An optimum pH value at 4.8 is found for $[Eu(deppa)_3]$, whereas $[Eu(meppa)_3]^{3-}$ is found to be more luminescent at pH 9.0. This phosphoryl series then nicely complements the maximum luminescence of $[Eu(dpa)_3]^{3-}$ at pH ~7.4.[21]

The competition between the complex formation and the protonation of the ligands usually prevents an acidic optimal luminescence, whereas, on the other hand, the competition between the formation of the complex and the formation of lanthanide hydroxides generally avoids basic optimal luminescence. Such difficulties are not encountered with $[Eu(deppa)_3]$, which keeps 75% of its maximal emission in the acidic range from pH 2.8 to pH 7.4, and with $[Eu(meppa)_3]^{3-}$, which still emits 75% of its maximal emission in a range from pH 5.2 to a fairly basic value of 10.4.

The modifications of the absorptions of the complexes as a function of pH correlates well with the absorption of the free ligands as a function of pH. The absorption of $[Eu(deppa)_3]$ at 266 nm remains fairly constant over the entire pH scale, whereas the absorption of $[Eu(meppa)_3]^{3-}$ at 268 nm significantly changes (see Figures S11 and S12 in the Supporting Information). The greater the acidity, the more $[Eu(meppa)_3]^{3-}$ absorbs (decreasing as pH increases). Therefore, the absorption behavior of $[Eu(meppa)_3]^{3-}$ is inverse to that of the emission. The obvious consequence of this behavior is that the quantum yield of $[Eu(meppa)_3]^{3-}$ benefits from both a better emission and a lower absorption at the optimal pH.

In addition, the integrated emission may be taken as an estimation of the quantum yield as a function of pH for $[Eu(deppa)_3]$. This is not the case for $[Eu(meppa)_3]^{3-}$, because its absorption considerably changes with pH; its quantum yield at low pH should decrease even more than the relative integrated emission of the luminescent lanthanide.

The effect of the pH under non-optimal conditions was further investigated by looking at the emission spectra of the $^5D_0 \rightarrow {}^7F_2$ hypersensitive transition of europium and its decay rate. The emission spectra of the $^5D_0 \rightarrow {}^7F_2$ hypersensitive transition of europium may indicate if the coordination is changing as a function of pH, whereas the lifetime analysis may indicate the presence of more than one emitting species.

Concerning $[Eu(deppa)_3]$, the hypersensitive transition does not seem to be affected by the change of pH. The emission just increases or decreases, but the shape is identical. The lifetimes at pH 4.8 and pH 7.4 are well-fitted with a mono exponential decay. A double exponential did not improve the residuals of the fittings. The lifetimes are presented in Table S2 in the Supporting Information. The mono exponential decay of the Eu emission is similar within experimental error at pH 4.8 and at pH 7.4. Therefore, the observed lifetime of 1.9 ms seems to be independent of the pH. If the loss in emission intensity is due to some decomplexation or to the formation of other species, these species are practically nonluminescent so that only the decrease of the amount of the tris species is observed. If the loss in emission intensity were due to some quenching of the Eu emission, the lifetime would be affected. The lifetime is consistent with the hypersensitive transition. No structural change in the tris complex is observed.

For $[Eu(meppa)_3]^{3-}$, the shape of the hypersensitive transition changes from the acidic pH values to the neutral and basic pH values (see Figure S13 in the Supporting Information). At pH 2, the transition is asymmetrically split, whereas at pH 11, the transition is symmetrical. The coordination of the Eu^{3+} ion to the $meppa^{2-}$ ligands is then affected in acidic solutions, and the species formed in acidic solutions is luminescent, even if to a lesser extent than the species that is encountered at the optimal basic pH.

Let us call the species found at pH 9 the *optimal species*, and the species formed in acidic solutions and exhibiting a disrupted inner coordination sphere the *acid-induced species*. The asymmetrical transition measured at pH 2 is then attributed to the acid-induced species and the symmetrical transition measured at pH 11 is attributed to the optimal species. The amount of acid-induced species at pH values of 5, 7, and 9 was estimated by fitting the normalized emission spectra of the europium hypersensitive transition at the considered pH, using a linear combination of the normalized emission spectra at pH 2 and pH 11. This procedure might allow one to retrieve the percentage of acid-induced species and optimal species present in the $^5D_0 \rightarrow {}^7F_2$ transitions at the intermediate pH values. Only 13% of the acid-induced species was fitted at pH 5, 8% at pH 7, and none at pH 9. This suggests that no residual inefficient acid-induced species remain at pH 9.

A lifetime analysis at pH values of 5, 7, and 9 was conducted similarly to $[Eu(deppa)_3]$. Here, the decay was found to be better fitted with double exponentials. A long lifetime of 2.0 ms and a shorter lifetime of 0.4 ms were found within the decay at all of the measured pH values. The percentage of the long lifetime was found to decrease, relative to the percentage of the short lifetime, as the pH decreases (see Table S2 in the Supporting Information). This result is in reasonable agreement with the fitting of the hypersensitive transition. The short lifetime species can thus be associated with the acid-induced species. The exact nature of this species is unknown; nevertheless, since the $[Eu(deppa)_3]$ complex did not show any structural change in the $^5D_0 \rightarrow {}^7F_2$ transitions as a function of pH, the monoethoxyphosphoryl functional group is almost certainly involved in such a change.

Photophysical Properties. The emission and excitation spectra of the ligands and their gadolinium, europium and terbium complexes were measured both at room temperature and at 77 K (see Figures 6 and 7). An aqueous KCl 0.1 M solution was used as a solvent, and 10% of glycerol was added for the low-temperature

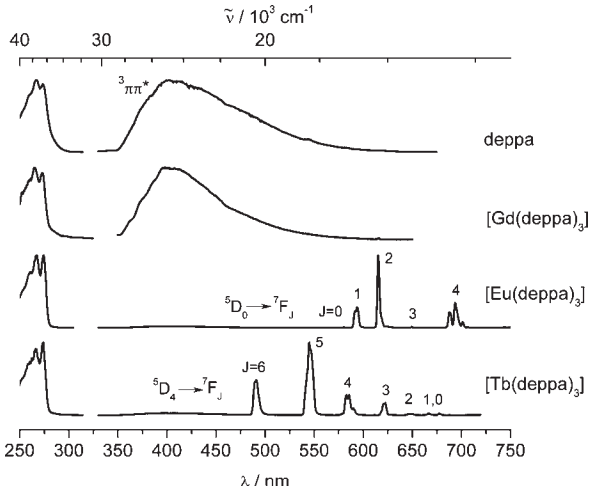

Figure 6. Excitation and emission spectra of deppa$^-$ and its complexes at 77 K. Conditions: 50 μs time delay; deppa$^-$ concentration = 1×10^{-4} M, in 0.1 M KCl aqueous solution; pH 4.8.

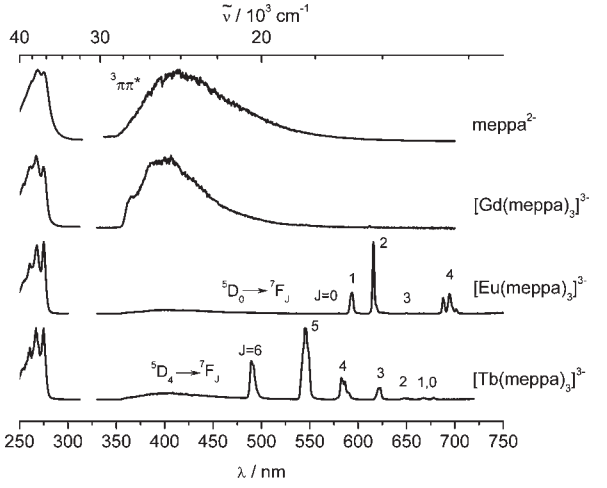

Figure 7. Excitation and emission spectra of meppa^{2-} and its complexes at 77 K. Conditions: 50 μs time delay; meppa^{2-} concentration = 1×10^{-4} M, in 0.1 M KCl aqueous solution; pH 9.0.

measurements. The pH was set at the optimal value for luminescence with 0.1 M HCl and 0.1 M NaOH.

Both ligands (deppa$^-$ and meppa^{2-}) exhibit a broad triplet emission band at low temperature (77 K), 50 μs after the pulsed excitation at 274 nm. This emission becomes slightly sharper upon coordination with a non-emissive lanthanide ion (here, gadolinium) and is strongly decreased when the energy can be transferred to a luminescent lanthanide ion (europium and terbium). An almost-complete disappearance is observed with deppa$^-$ complexes, and a faint remaining triplet emission is observed with the meppa^{2-} complexes. This already shows a better energy transfer from the deppa$^-$ triplet state to the lanthanide ion than from the meppa^{2-} to the same lanthanide ion.

The excitation spectra are all located on the absorption range of the ligands and have similar shapes as the absorption spectra, meaning that the energy is indeed absorbed by the ligands and transferred to the lanthanide (antenna effect).

A usual broadening of the emission peaks of the luminescent cations and a disappearance of the remaining emission from the triplet state is experienced between the emission spectra of the europium and terbium complexes measured at room temperature and at low temperature, but no other significant difference is observed.

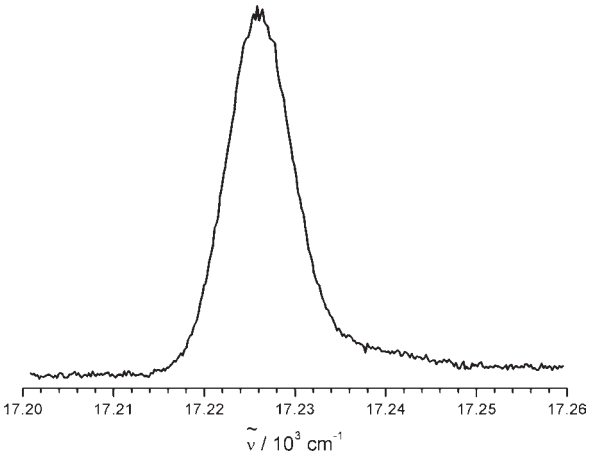

Figure 8. High-resolution excitation spectrum of the $^5D_0 \leftarrow {}^7F_0$ transition for the emission at 615 nm. Conditions: 12 K, 5×10^{-3} M aqueous solution of [Eu(deppa)$_3$], pH 4.8 with 10% glycerol. Maximum observed at 17 226 cm^{-1} (580.53 nm), half-width of 8.4 cm^{-1}.

The emissions of europium and terbium were then characterized at room temperature by their lifetime analysis, as well as with the determination of their quantum yields.

The fitting of [Eu(deppa)$_3$] is mono exponential and the fitting of [Eu(meppa)$_3$]$^{3-}$ is a double exponential decay, exhibiting a long lifetime and a short lifetime. The mono exponential lifetime and the long double exponential lifetime are in the millisecond range. They are fairly similar, with values of 1.9 ms for [Eu(deppa)$_3$] and 2.0 ms for [Eu(meppa)$_3$]$^{3-}$. The shorter second lifetime of [Eu(meppa)$_3$]$^{3-}$ is 0.4 ms. These lifetimes are in good agreement with typical values for filled and hydrated coordination sphere. As a comparison, the standard [Eu(dpa)$_3$]$^{3-}$ complex exhibits a long lifetime (~1.7 ms) and a short lifetime (~0.3 ms) that is attributed to the tris-hydrated [Eu(dpa)$_2$]$^-$ species.[21]

When it comes to the terbium emission, [Tb(deppa)$_3$] exhibits a high lifetime of 2.4 ms, whereas [Tb(meppa)$_3$]$^{3-}$ shows a lifetime of 1.4 ms. In addition, the lifetime of [Tb(deppa)$_3$] remains unchanged upon cooling to 77 K, indicating that no significant vibrationally assisted back transfer is occurring from the Tb^{3+} ion back to the ligand. In comparison, [Eu(deppa)$_3$] has a higher lifetime of 2.3 ms at 77 K versus 1.9 ms at room temperature.

The number of water molecules in the first coordination sphere (q) was determined for the europium complexes by measuring the lifetimes both in H_2O and D_2O. Using eqs 3a and 3b, along with $\alpha = 0.31$ ms^{-1} and $A = 1.11$ ms, and zero XH oscillators in the first coordination sphere, no water molecules are found (see Table S3 in the Supporting Information).

A high-resolution excitation spectrum of the $^5D_0 \leftarrow {}^7F_0$ transition was performed for the europium tris(diethoxyphosphoryl picolinate). A 5×10^{-3} M aqueous solution of [Eu(deppa)$_3$], pH 4.8, with 10% glycerol added was frozen at 12 K and the high-resolution excitation spectrum recorded for the emission of the $^5D_0 \rightarrow {}^7F_2$ transition (see Figure 8).

A single peak is measured with a maximum at 17 226 cm^{-1} and a half-width of 8.4 cm^{-1}. This clearly demonstrates that the emitting

Table 4. Radiative and Observed Lifetimes (τ), Sensitized and Intrinsic Quantum Yields (Φ), and Sensitization Efficiencies (η) (Concentration = 1.0×10^{-4} M, 298 K under Optimal Conditions (see above); Estimated Errors = 10%)

	τ_{obs} (ms)	τ_r (ms)	$\Phi_{L,Ln}$	$\Phi_{Ln,Ln}$	η_{sens}
$[Eu(dpa)_3]^{3-}$ [a]	1.7	4.4	0.24	0.39	0.61
$[Tb(dpa)_3]^{3-}$	2.1	n.d.	0.22	n.d.	n.d.
$[Eu(deppa)_3]$ [b]	1.9	6.2	0.15	0.31	0.49
$[Tb(deppa)_3]$ [b]	2.4	n.d.	0.40	n.d.	n.d.
$[Eu(meppa)_3]^{3-}$ [c]	2.0	5.2	0.08	0.38	0.21
$[Tb(meppa)_3]^{3-}$ [c]	1.4	n.d.	0.14	n.d.	n.d.

[a] From ref 24. [b] pH = 4.8. [c] pH = 9.0.

Eu^{3+} ion has only one defined coordination geometry. Hence, the 1:3 complex is the major species and exhibits only one geometry in the case of $deppa^-$ as the ligand.

The quantum yields were finally calculated relative to the europium and terbium trisdipicolinate emission. The europium emission spectra were then used to calculate the radiative lifetimes, intrinsic quantum yields, and sensitization efficiencies, according to eqs 2a−c (see Table 4).

The $deppa^-$-sensitized emissions are always better than the $meppa^{2-}$-sensitized ones. The europium emission is more efficient first in $[Eu(dpa)_3]^{3-}$, then in $[Eu(deppa)_3]$ and weaker in $[Eu(meppa)_3]^{3-}$. The quantum yield between the $[Eu(deppa)_3]$- and the $[Eu(meppa)_3]^{3-}$-sensitized europium emission decreases by a factor of ∼2. When looking at the intrinsic quantum yields and sensitization efficiencies, the difference between $[Eu(deppa)_3]$ and $[Eu(meppa)_3]^{3-}$ is mainly due to the better sensitization efficiency of the $deppa^-$ ligand. Almost half of the absorbed photons are transferred to the lanthanide with $deppa^-$, versus only 21% with $meppa^{2-}$. In addition, the slight increase in intrinsic quantum yields from $[Eu(deppa)_3]$ to $[Eu(meppa)_3]^{3-}$ is not sufficient to compensate for the lower sensitization of the $meppa^{2-}$ ligand.

Concerning the terbium emissions, better efficiency is found in $[Tb(deppa)_3]$. A high quantum yield of 40% is reached, which is almost twice the $[Tb(dpa)_3]^{3-}$-sensitized emission. $[Tb(meppa)_3]^{3-}$ is also better than the corresponding europium emission, with a fair 14% quantum yield.

Very high terbium quantum yields (up to 95%) have already been measured in aqueous solution with functionalized 2,6-bispyrazolyl-pyridine derivatives.[26] Such ligands form 1:1 complexes with lanthanide ions. The replacement of the carboxylate coordinating groups in such 2,6-bispyrazolyl-pyridine derivatives with phosphonates was also undertaken and yielded lower quantum yields and higher lifetimes.[16] Despite the unique example of carboxylate-functionalized 2,6-bispyrazolyl-pyridine derivatives, quantum yields higher than those of the luminescent $[Ln(dpa)_3]^{3-}$ complexes in aqueous solutions are seldom encountered. Thus, a quantum yield of 40% remains high, compared to the average quantum yields in aqueous solutions.

Although no simple calculation of the radiative lifetime of terbium luminescence is known, some reasonable assumptions considering the efficiency of the high $[Tb(deppa)_3]$ luminescence can be undertaken, based on the previous discussion on lifetimes. Because cooling the sample seems to have no effect on the lifetime, the energy is lost by other means than back transfer. Hence, the portion of the sensitization efficiency coming from the ligand-to-metal energy-transfer efficiency should be rather high (higher than with usual values for which back transfer is taking place). The limiting factor of this sensitization efficiency might then be the intersystem crossing of the ligand from singlet to triplet. Nevertheless, no indication considering the intrinsic quantum yield is available, so that it is difficult to discuss whether the high quantum yield is the result of a high sensitization and an average intrinsic quantum yield or an average sensitization with a good intrinsic quantum yield.

Rationalizing the lower quantum yield of the $meppa^{2-}$ complexes, compared to the corresponding $deppa^-$ ones, should also be performed carefully, since very few data are available to confirm the assumptions. A similar observation was performed, comparing helicate structures formed with monoethoxyphosphoryl or dihydroxyphosphoryl groups replacing the carboxylates.[14] There, the dihydroxy helicate complex usually had a lower quantum yield than the monoethoxy analogue. The attempted explanation was a higher hydrophilicity of dihydroxy groups, which could generate more hydrogen bonding with proximate water molecules. However, a simple structure-based discussion might yield some further interesting considerations. The structural difference between the two ligands is the replacement of one ethoxy group on the phosphoryl with a hydroxyl group. Independently of any consideration on the coordination mode of the phosphoryl group, the removal of one ethoxy has two direct consequences. First, it relaxes some steric hindrance in the complex, and furthermore introduces an additional negative charge, which might allow a harder interaction between the phosphoryl and the cation and, thus, should shorten the distance between the ligand and the metal ion, compared to the interaction with an uncharged coordination site. Therefore, the major difference between the two complexes ($[Ln(deppa)_3]$ or $[Ln(meppa)_3]^{3-}$) is certainly a slightly different distance and tilt between the ligands and the lanthanide ion. Looking at the triplet state energies in Figures 6 and 7, the position is fairly similar, so that the energy gap between the triplet state and the excited levels of either europium or terbium should be similar for both ligands. In addition, as already partly proposed by Chauvin et al.,[14] the negative charge might induce some other effects (for example, on the surrounding solvent), which might favor quenching and impact the transfer rate from the ligand toward the lanthanide ion, the deactivation of the excited state of the ligand, and the different deactivations of the lanthanide ion.

CONCLUSIONS

6-Diethoxyphosphoryl picolinic acid, 6-monoethoxyphosphoryl, and 6-dihydroxyphosphoryl picolinic acid were synthesized and used as ligands for luminescent lanthanide complexes. The formation of lanthanide complexes was studied and showed comparable stabilities within the phosphoryl series, except for the dihydroxy ligand, because of a prompt precipitation when a lanthanide cation is added. Similar to the literature, the phosphoryl derivatives tend to increase the stability constants, compared to a carboxylate analogue.[8,9] A nice complementary behavior was shown between dpa^{2-}, $deppa^-$, and $meppa^{2-}$ complexes, which have respective maximum emission intensities in neutral (pH 7.4), acidic (pH 4.8), and basic (pH 9.0) media. Hence, an uncommonly low pH value of 3 still allows a good emission of Eu tris-$deppa^-$ complex, whereas an uncommonly high pH of 10 still allows a good emission of Eu tris-$meppa^{2-}$ complex. This pH behavior was partly explained for $[Eu(meppa)_3]^{3-}$ by pointing at a change in the shape of the hypersensitive $^5D_0 \rightarrow {}^7F_2$ europium transition that indicates a change in the inner coordination sphere at low pH. The presence of a mixture of the disturbed,

possibly protonated complex species, together with the more efficiently luminescent tris complex under acidic conditions, up to neutral conditions, was also confirmed by lifetime analysis.

For the europium tris-deppa$^-$ complex, a fair quantum yield of 15% was measured at the optimal pH. It was found to be much more important for Tb tris-deppa$^-$, with a quantum yield of 40%. On the other hand, Eu and Tb tris-meppa^{2-} complexes have lower quantum yields, with 8% and 14%, respectively. The lifetimes in deuterated water precluded the presence of water molecules in the first coordination sphere of deppa$^-$ and meppa^{2-} complexes. A high- resolution excitation spectrum of the $^5D_0 \leftarrow {}^7F_0$ transition at low temperature also demonstrated that the Eu^{3+} ion has a single geometry with deppa$^-$ as the ligand. The estimations of the radiative lifetimes and intrinsic quantum yields of the europium complexes suggest a better emission efficiency of the europium in $[Eu(meppa)_3]^{3-}$, compared to $[Eu(deppa)_3]$; however, the low sensitization efficiency significantly decreases the quantum yield, so that $[Eu(deppa)_3]$ is a better emitter than $[Eu(meppa)_3]^{3-}$. This significant decrease in lanthanide quantum yield from the sensitization with a deppa$^-$ ligand to the sensitization with a meppa^{2-} ligand might be rationalized by plausible structural differences induced by the negative charge and the less-hindered ligand, as well as by possible increased solvent interactions in the charged and less-hindered meppa^{2-} complex favoring nonradiative deactivations.

Comparatively to the dipicolinic acid complexes, it is obvious that the 6-phosphoryl picolinic ligands are, to some extent, more intricate. This may favor the simpler dpa^{2-} as standards for quantum yields, for example; however, it opens many perspectives for applications and investigations based on deppa$^-$ and meppa^{2-} structures.

This class of ligands might have potential applications as probes or sensors as well as in color reproduction domains because of their interesting pH complementarities, of the potential sensing abilities of the monoethoxyphosphoryl group (which are yet to be explored), and of the high quantum yield of the terbium diethoxyphosphoryl complex.

■ ASSOCIATED CONTENT

Supporting Information. ^{31}P NMR chemical shifts of the three ligands protonated species, lifetimes evolution as a function of pH, water molecules in first coordination sphere, absorption spectra as a function of pH, species distribution diagrams, UV−vis titration of meppa^{2-} with Eu^{3+} and the corresponding species distribution as a function of Eu^{3+}-to-ligand ratio, ^{31}P NMR spectra of H_2meppa in D_2O titrated with Lu^{3+}, absorption of the complexes as a function of pH, emission spectra of $[Eu(meppa)_3]^{3-}$ at different pH, ESI-TOF-MS spectra of $[Eu(deppa)_3]$ in water. This material is available free of charge via the Internet at http://pubs.acs.org.

■ AUTHOR INFORMATION

Corresponding Author

*E-mail addresses: anne-sophie.chauvin@epfl.ch (A.-S.C.), julien.andres@epfl.ch (J.A.).

■ ACKNOWLEDGMENT

We thank Prof. Jean-Claude G. Bünzli for hosting us in his laboratory, Mr. Frédéric Gumy and Dr. Svetlana Eliseeva for high-resolution excitation measurements, and Prof. Roger D. Hersch for providing financial support. This research is supported through grants from the Swiss National Science Foundation (FNS No. 126757).

■ REFERENCES

(1) Bünzli, J.-C. G.; Piguet, C. Organized lanthanide-containing molecular systems for light conversion. In *Encyclopedia of Materials: Science and Technology*; Buschow, K. H. J., Cahn, R. W., Flemings, M. C., Ilschner, B., Kramer, E. J., Mahajan, S., Eds.; Elsevier Science, Ltd.: Oxford, U.K., 2001; pp 4465−4476.

(2) Bünzli, J.-C. G.; Piguet, C. *Chem. Soc. Rev.* **2005**, *34*, 1048–1077.

(3) Bünzli, J.-C. G.; Comby, S.; Chauvin, A.-S.; Vandevyver, C. D. B. *J. Rare Earths* **2007**, *25*, 257–274.

(4) dos Santos, C. M. G.; Harte, A. J.; Quinn, S. J.; Gunnlaugsson, T. *Coord. Chem. Rev.* **2008**, *252*, 2512–2527.

(5) D'Aléo, A.; Picot, A.; Beeby, A.; Gareth Williams, J. A.; Le Guennic, B.; Andraud, C.; Maury, O. *Inorg. Chem.* **2008**, *47*, 10258–10268.

(6) Latva, M.; Takalo, H.; Mukkala, V. M.; Matachescu, C.; Rodriguez-Ubis, J.-C.; Kankare, J. *J. Lumin.* **1997**, *75*, 149–169.

(7) Picot, A.; D'Aleo, A.; Baldeck, P. L.; Grichine, A.; Duperray, A.; Andraud, C.; Maury, O. *J. Am. Chem. Soc.* **2008**, *130*, 1532–1533.

(8) Andres, J.; Chauvin, A.-S. *Eur. J. Inorg. Chem.* **2010**, 2700–2713.

(9) Binnemans, K. *Chem. Rev.* **2009**, *109*, 4283–4374.

(10) Lukes, I.; Kotek, J.; Vojtisek, P.; Hermann, P. *Coord. Chem. Rev.* **2001**, *216−217*, 287–312.

(11) Táborský, P.; Svobodová, I.; Lubal, P.; Hnatejko, Z.; Lis, S.; Hermann, P. *Polyhedron* **2007**, *26*, 4119–4130.

(12) Kubícek, V.; Rudovský, J.; Kotek, J.; Hermann, P.; Vander Elst, L.; Muller, R. N.; Kolar, Z. I.; Wolterbeek, H.; Peters, J. A.; Lukes, I. *J. Am. Chem. Soc.* **2005**, *127*, 16477–16485.

(13) Rehor, I.; Kubícek, V.; Kotek, J.; Hermann, P.; Száková, J.; Lukes, I. *Eur. J. Inorg. Chem.* **2011**, 1981–1989.

(14) Chauvin, A.-S.; Comby, S.; Baud, M.; De Piano, C.; Duhot, C.; Bünzli, J.-C. G. *Inorg. Chem.* **2009**, *48*, 10687–10696.

(15) Comby, S.; Imbert, D.; Chauvin, A.-S.; Bünzli, J.-C. G.; Charbonnière, L. J.; Ziessel, R. F. *Inorg. Chem.* **2004**, *43*, 7369–7379.

(16) Nono Katia, N.; Lecointre, L.; Regueiro-Figueroa, M.; Platas-Iglesias, C.; Charbonnière, L. J. *Inorg. Chem.* **2011**, *50*, 1689–1697.

(17) Kotková, Z.; Pereira, G. A.; Djanashvili, K.; Kotek, J.; Rudovský, J.; Hermann, P.; Vander Elst, L.; Muller, R. N.; Geraldes, C. F. G. C.; Lukes, I.; Peters, J. A. *Eur. J. Inorg. Chem.* **2009**, *2009*, 119–136.

(18) Pangborn, A. B.; Giardello, M. A.; Grubbs, R. H.; Rosen, R. K.; Timmers, F. J. *Organometallics* **1996**, *15*, 1518–1520.

(19) Schwarzenbach, G. *Complexometric Titrations*; Chapman & Hall: London, 1957.

(20) Gampp, H.; Maeder, M.; Meyer, C. J.; Zuberbühler, A. D. *Talanta* **1985**, *23*, 1133–1139.

(21) Chauvin, A.-S.; Gumy, F.; Imbert, D.; Bünzli, J.-C. G. *Spectrosc. Lett.* **2004**, *37*, 517; Erratum, **2007**, *40*, 193.

(22) Werts, M. H. V.; Jukes, R. T. F.; Verhoeven, J. W. *Phys. Chem. Chem. Phys.* **2002**, *4*, 1542–1548.

(23) Supkowski, R. M.; Horrocks, W. DeW., Jr. *Inorg. Chim. Acta* **2002**, *340*, 44–48.

(24) Gassner, A.-L.; Duhot, C.; Bünzli, J.-C. G.; Chauvin, A.-S. *Inorg. Chem.* **2008**, *47*, 7802–7812.

(25) Franz, R. G. *AAPS PharmSci.* **2001**, *3*, No. Article 10.

(26) Brunet, E.; Juanes, O.; Sedano, R.; Rodriguez-Ubis, J.-C. *Photochem. Photobiol. Sci.* **2002**, *1*, 613–618.